

# HORIZONTAL TRANSPORT OF THE REGOLITH, MODIFICATION OF FEATURES, AND EROSION RATES ON THE LUNAR SURFACE

R. ARVIDSON, R. J. DROZD, C. M. HOHENBERG,  
C. J. MORGAN, and G. POUPEAU

*McDonnell Center for the Space Sciences, Washington University, St. Louis, Mo., U.S.A.*

**Abstract.** New lunar soils, freshly deposited as impact ejecta, evolve into more mature soils by a complex set of processes involving both near-surface effects and mixing. Poor vertical mixing statistics and interregional exchange by impact ejection complicate the interpretation of soil maturation. Impact ejecta systematics are developed for the smaller cratering events which, with cumulative crater populations observed in young mare regions and on Copernicus ejecta fields, yield rates and a range distribution for the horizontal transport of material by impact processes. The deposition rate for material originating more than 1 m away is found to be about  $8 \text{ mm m.y.}^{-1}$ . Material from 10 km away accumulates at a rate of about  $0.08 \text{ mm m.y.}^{-1}$ , providing a steady influx of foreign material. From the degradation of boulder tracks, a rate of  $5 \pm 3 \text{ cm m.y.}^{-1}$  is computed for the filling of shallow lunar depressions on slopes. Mass wastage and downslope movement of bedrock outcroppings on Hadley Rille seems to be proceeding at a rate of about  $8 \text{ mm m.y.}^{-1}$ . The Camelot profile is suggestive of a secondary impact feature.

## 1. Introduction

A cratering event large enough in size to penetrate the lunar regolith will bring some material to the lunar surface for the first time. A number of parameters have been suggested to describe how this 'fresh soil' evolves or matures with time. Among the proposed 'maturity indicators' are (1) the abundance of glassy agglutinates which are formed by meteoroid impact (Clanton *et al.*, 1972; McKay *et al.*, 1972), (2) the soil particle size distribution (McKay *et al.*, 1972), (3) the fraction of grains with a high density of solar flare heavy particle tracks (Croaz *et al.*, 1972), and (4) the fraction of grains with amorphous, radiation-damaged surfaces (Maurette and Price, 1975).

Major questions arise, however, as soon as one tries to interpret these 'maturation parameters', measured in individual soil samples, in terms of an age for a regolithic unit excavated from depth and deposited as a blanket of fresh material. Foremost among these are uncertainties in obtaining representative samples and in maintaining the integrity of a regolithic unit, i.e., the problem of soil mixing involving both the vertical and horizontal components. Rates for vertical mixing have been treated by Monte Carlo cratering techniques (Arnold, 1974; Gault *et al.*, 1974). We discuss in this paper the impact these results have on the interpretation of maturity parameters. The role of horizontal transport as a regolithic mixing process has been explored to a lesser degree. Ages inferred for a regolithic unit by means of soil maturity parameters can be in error if significant amounts of material have been interchanged with surrounding, and perhaps older, regions. We therefore also examine horizontal components of mixing in the regolith by using crater and ejecta distribution modeling for impact events.

## 2. Vertical Mixing: The Sampling Problem

Monte Carlo techniques demonstrate that the rate of vertical mixing by meteoroid bombardment decreases very rapidly with depth. The predicted time for turnover (50% probability) to a depth of several centimeters is on the order of tens of millions of years (Arnold, 1974; Gault *et al.*, 1974). Since solar wind interactions, agglutinate formation, and many other phenomena that age a soil occur only in the outermost millimeter, the 'mixing zone' (Gault *et al.*, 1974), it follows that a single soil sample, scooped to a depth of several centimeters from a fresh ejecta blanket, will give maturation indices that are only statistically related to the age of the blanket. The stochastic nature of vertical mixing becomes evident when one observes that the characteristic mixing time to the scooping depth for soil samples is on the same order of magnitude as the age (several tens of millions of years) of dateable ejecta blankets sampled during the missions. Consequently, large statistical variations in the maturity parameters of otherwise identical soil samples are expected. In addition, sampling to different depths can also result in differences in the apparent degree of maturity.

Figure 1 displays two properties used to describe soil maturity: The fraction of grains with track densities in excess of  $10^8 \text{ t cm}^{-2}$  and the solar wind  $^{36}\text{Ar}$  content. Both of these are properties that develop in the near-surface region. If there were no mixing, newly-exposed 'zero-age' material would plot at the origin. As maturation proceeds and the soil properties change in their characteristic way, the locus of points would define a concordancy track, moving first from the origin toward the upper right (line O-A), then, as the grains attain a saturated solar flare track dose, moving horizontally to the right (line A-B). Actual sample data, however, do not behave in

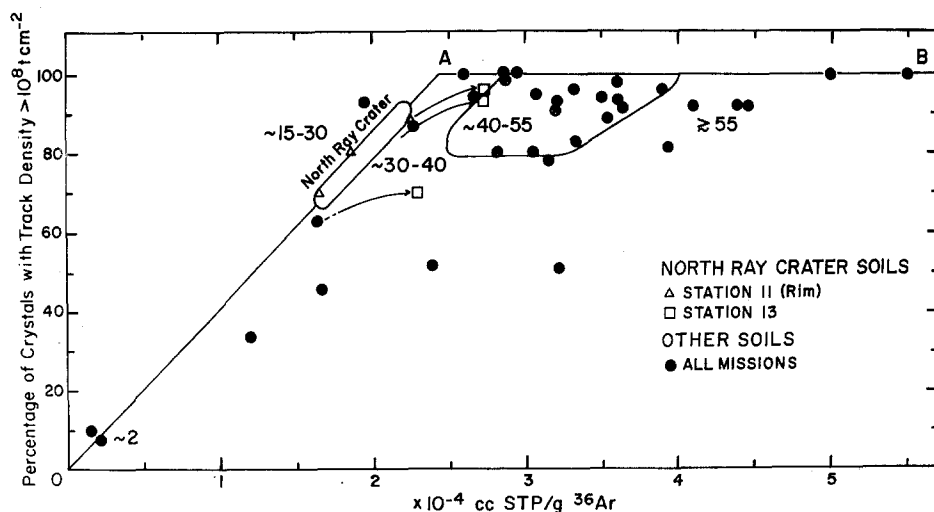


Fig. 1. Bulk average  $^{36}\text{Ar}$  content and selected percentages of track-rich crystals in surface soils from Apollo 11-17 sites and Luna 16 core. The numbers in the figure refer to the percentages of glassy agglutinates (90-150 $\mu$  range). Arrows indicate evolutionary tracks for North Ray Station 13 soils due to intermixing with a more mature component.

this way. Instead, they are spread over most of the plane to the right of lines O-A and A-B. Displacements from the model soil evolution track are probably due to both artificial variations in maturity parameters, caused by different scooping depths, and natural variations in these parameters due to the stochastic nature of soil mixing. Impact gardening by the larger (centimeter-sized) events mixes in 'zero-age' material from depth, diluting in a quite random way the properties which define soil maturity. Both processes introduce young components which move the individual points toward the origin and off the concordancy line in Figure 1.

### 3. The North Ray Story

Figure 2 is a plot of agglutinate content versus the age of soil emplacement. In this figure the only soils plotted are those that were collected from the ejecta blankets of dateable craters (Arvidson *et al.*, 1975). Thus, the age of deposition of the bulk of the soil unit is known and correlations can be tested for increase in agglutinate content with time. The fundamental assumption is that agglutinates are non-existent in fresh material excavated from beneath the regolith. A great deal of scatter is present, again probably reflecting sampling differences and the stochastic nature of local regolith mixing.

Samples collected from the continuous ejecta blanket of North Ray Crater (Stations 11 and 13) are plotted in Figures 1 and 2 as triangles and squares. The Station 11 samples, from the rim of the crater (triangles), scatter along the segment O-A in

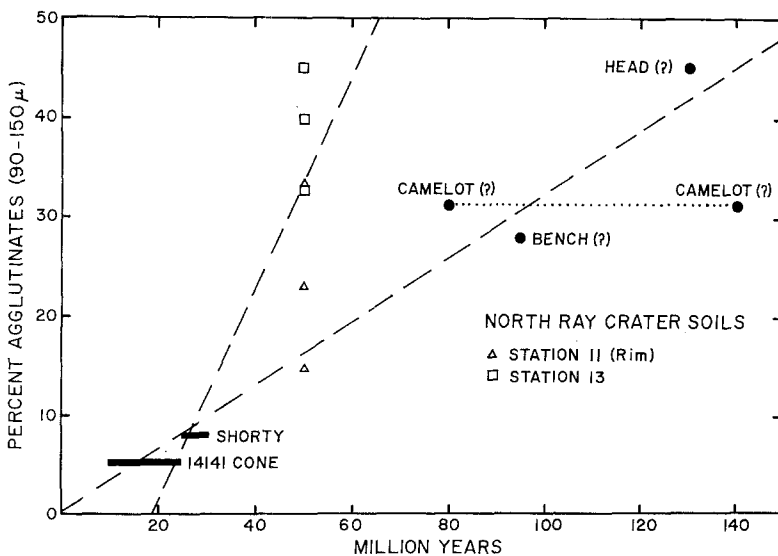


Fig. 2. Percentages of glassy agglutinates in the 90-150 $\mu$  range for some regolith units. Glassy agglutinate data from McKay and co-workers (tabulated in Heiken, 1974); regolith unit ages are from Arvidson *et al.* (1975). The two dashed lines are ranges for possible fits to the data, illustrating the large degree of uncertainty involved. As indicated by question marks, ages for Head, Camelot, and Bench craters are still uncertain.

Figure 1, reflecting real variations in the average exposure history of the individual soils sampled. Corresponding variations are found in Figure 2. These variations have no information content for regional evolution except to demonstrate in a rough way the kind of statistical variations one is likely to find among individual samples of this rather restricted size. They reflect varying dilutions with immature or 'zero-age' soils located near the origin.

Samples from Station 13 (squares) plot to the right of the line O-A in Figure 1 even though the upper regolith at the two stations was deposited simultaneously. We suggest inter-mixing with a more *mature* regolithic component may have occurred for the Station 13 samples. The same conclusion is drawn from the data of Figure 2; the

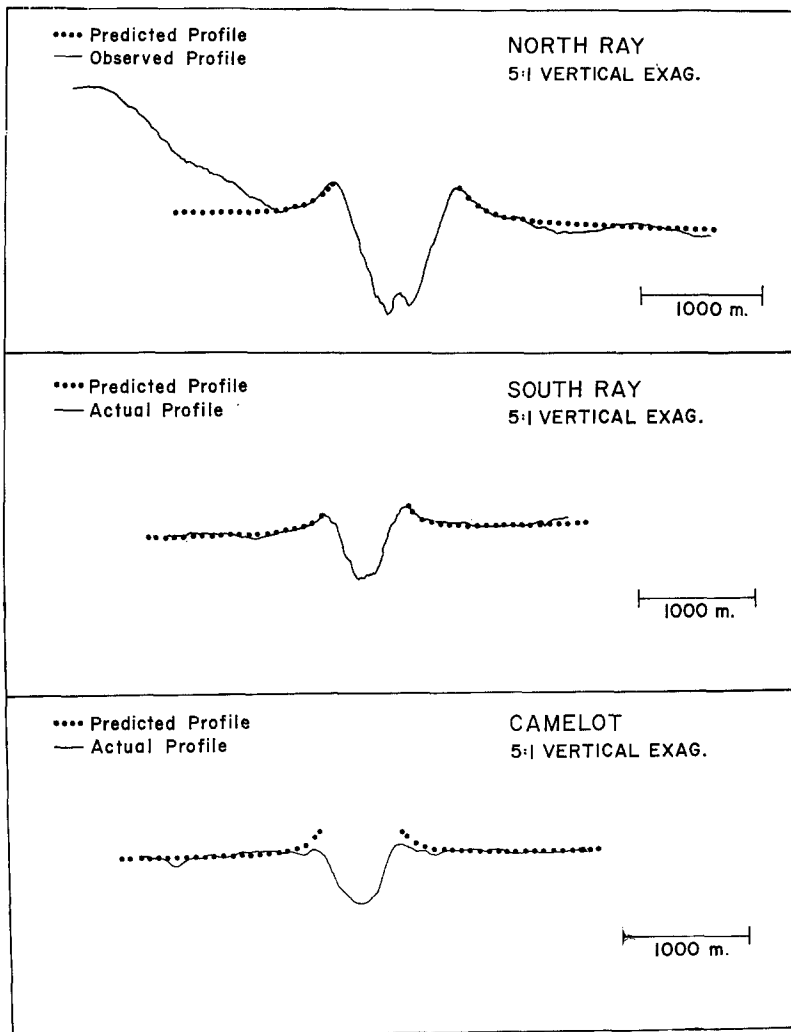


Fig. 3. Profiles measured for North Ray, South Ray, and Camelot Craters are shown in solid lines and profiles predicted by Equation (4) for fresh hypervelocity impact features are shown by the dots.

agglutinate content is higher for the Station 13 samples. Rare gas data furnish additional supportive evidence. Exposure ages, based upon spallation-produced  $^{38}\text{Ar}$ , are commensurate with the 50-m.y. age of North Ray Crater for the Station 11 soils, while the unshielded Station 13 soils yield exposure ages of 80–90 m.y. (Bogard and Nyquist, 1973; Kirsten *et al.*, 1973), strongly suggesting contamination with more mature components. The North Ray ejecta blanket at Station 11 is about 50 m thick, dropping to about 3 m at Station 13, still too thick to allow intermixing with underlying material by the normal gardening processes. Some other mixing mechanism must be at work. Incorporation of the underlying regolith may have occurred upon deposition of the blanket due to stirring by secondary impacts in a manner similar to that proposed for large ( $> 1$  km) events by Oberbeck *et al.* (1974), although inter-unit mixing by the horizontal exchange of material after the North Ray event may be an alternative mechanism.

Figure 3 shows profiles for North Ray, South Ray, and Camelot Craters and the profiles for ejecta topography predicted on the basis of ejecta distribution models developed later in this paper. Both North Ray and South Ray Craters, as their names imply, are surrounded by bright haloes and rays, features commonly used to distinguish craters as hypervelocity impacts rather than low velocity secondary cratering events (Mutch, 1972). Fits to predicted shapes are good for both craters, while Camelot is noticeably more subdued. South Ray can be dated at 2 m.y. old and North Ray at 50 m.y. old by concordant sample cosmic ray exposure ages (Arvidson *et al.*, 1975). Dating of Camelot presents more of a problem because exposure age concordancy is not found. Two groupings of ages exist for samples collected from Camelot, those around 80 m.y. and those around 140 m.y. (Arvidson *et al.*, 1975). If either the 80 or 140 m.y. age represents the Camelot cratering event, it is difficult to reconcile the subdued shape as being due to erosion when compared to North Ray, which is pristine in shape and within a factor of three in age of 140 m.y. The high density of blocks in the vicinity of Camelot (Muehlberger *et al.*, 1973) also argues for an initially subdued starting profile, since it would be difficult to remove the needed  $\sim 20$  m of material without destroying the block population. We tentatively conclude that Camelot Crater is the result of a lower velocity secondary impact event.

#### 4. Rim Erosion at Hadley Rille

Three of the Apollo 15 samples, taken from boulder fields near the rim of Hadley Rille, have cosmic ray exposure ages near 100 m.y. (15535, 15555, 15595; Arvidson *et al.*, 1975). According to transcripts at the site and verified by surface photography, little, if any, regolith covers the bedrock in this region. Due to the old age of Hadley Rille, which could be contemporaneous with magmatic flows in the region, 100 m.y. apparent ages for these rocks are probably not due to the static accumulation of spallation rare gases, but rather may be due to a secular equilibrium reflecting both accumulation and erosion. From the physical constraints imposed by the bedrock body and from the lack of appreciable regolith cover, it is unlikely that these samples could have

had complex exposure histories. Accepting such boundary conditions, we can compute an average erosion rate for the exposed bedrock.

For a constant rate of erosion, the time a given sample spends at each increment of depth will, in general, be a constant. The total accumulation of spallation rare gases in the sample can be found by integrating this exposure over all depths in the form

$$[83]_s = \int_0^{\infty} \frac{{}^{83}\text{P}(X)}{R} dx, \quad (1)$$

where  $[83]_s$  is  ${}^{83}\text{Kr}$  produced in spallation,  ${}^{83}\text{P}(X)$  is the rate of production of  ${}^{83}\text{Kr}$  as a function of depth, and  $R = dx/dt$  is the erosion rate for the exposed rock surface. The production rate at the surface  ${}^{83}\text{P}(0)$  is known from the equilibrium concentration of 0.210 m.y.  ${}^{81}\text{Kr}$  and the ratio of production rates,  ${}^{81}\text{P}/{}^{83}\text{P}$ , measured for these samples (Marti and Lightner, 1972; Alexander *et al.*, 1973; Drozd *et al.*, 1974). The depth variation of the production rate can be adequately treated by using depth variations for various cosmogenic nuclides computed by Reedy and Arnold (1972). Uncertainties about the excitation functions of the specific reactions involved are evaluated by computing apparent erosion rates for the full range of energetics; soft, with a production rate profile similar to that for  ${}^{37}\text{Ar}$ , and hard, with a production rate profile similar to that of  ${}^3\text{H}$  (see Reedy and Arnold, 1972). Equation (1) can be numerically integrated, yielding an erosion rate of  $8 \pm 3$  mm m.y.<sup>-1</sup> with error limits predominantly reflecting uncertainties in  ${}^{83}\text{P}(X)$ . It should be pointed out that this erosion rate applies to mass wastage, spalling, and cracking with subsequent downslope movement of debris to form a talus deposit in the rille. It should not be compared with previously computed erosion rates for rock surfaces (Behrmann *et al.*, 1973; Crozaz *et al.*, 1974). If most removal from the bedrock samples takes place by large blocks spalling off bedrock and rolling downhill, then values computed for the erosion rates could be affected by recent shielding changes.

## 5. The Filling of Shallow Depressions: Rates of Boulder Track Degradation

Another method of setting boundary conditions for soil mixing rates is to estimate rates of fill-in of shallow depressions, like boulder tracks. The Apollo 17 Station 6 boulder, roughly 15 m by 8 m in size, apparently rolled down the North Massif, leaving a track nearly 2 km long which is still visible. The boulder itself rests on a slope of roughly 12° but the track remains visible upslope where the grade is about 25°, suggesting that downslope mass movement has not been an overriding factor in the degradation of these boulder tracks since boulder emplacement. Since we know the time of boulder emplacement, we can set an upper limit on the rate of fill-in of meter-sized depressions, in this case on 10–25° slopes. An estimate of the original track depth can be made by assuming a spherical boulder 12 m in diam and a track width of 8.5 m (Mitchell *et al.*, 1973), which yields an initial depth of about 1.8 m. This depth is in approximate agreement with the penetration expected based upon a bearing

strength estimated from the depth of the Rover tracks (Mitchell *et al.*, 1973). On the basis of concordant cosmic ray exposure ages, Arvidson *et al.* (1975) conclude that the boulder has been at the bottom of the massif for 22 m.y. The track is still visible so that an upper limit for the rate of track fill-in appears to be about  $8 \text{ cm m.y.}^{-1}$ .

Similarly, a lower limit can be set from the Apollo 17 Station 7 boulder, which has no track. Because of the similarity in composition and structure with other boulders at the base of the massif (Muehlberger *et al.*, 1973), many of which have tracks leading upslope, this boulder was most likely derived from a source region high on the North Massif. One can estimate the initial track depth, assuming it had one, from the size of the boulder. The boulder mass scales as the cube of the linear dimension; the cross sectional area scales as the square. Therefore, one would expect that regolith penetration depth would be roughly proportional to the linear dimension. Comparing the Station 7 boulder with the Station 6 boulder, we estimate an original track depth of about 45 cm for the Station 7 boulder. For emplacement 28 m.y. ago (Arvidson *et al.*, 1975), a lower limit of about  $2 \text{ cm m.y.}^{-1}$  is set. We therefore estimate that shallow depressions in the lunar surface are filled at an apparent rate bracketed by these two limits,  $5 \pm 3 \text{ cm m.y.}^{-1}$ . Two mechanisms are probably responsible for track degradation: downhill mass movements, and cratering, which tends to wear down track edges and preferentially fill in the track proper. It is difficult to separate relative magnitudes of slope-related mass movements (i.e., non-impact-related) from cratering effects.

## 6. Horizontal Mixing: Source Distributions and Rates of Deposition

Whether by Monte Carlo modeling or empirical determinations of boulder track fill-in, the question still remains as to where the interchanged or deposited material came from before being transported to the sampled site. In order to adequately treat horizontal transport and estimate its distribution as a function of range, it is necessary to develop ejecta distribution models for cratering events of the scale that mixes material over distances ranging from meters to kilometers. Because of the low influx rate for large projectiles, we limit the present calculations to craters less than tens of kilometers in size. McGetchin *et al.* (1973) have developed semi-empirical ejecta systematics for large lunar cratering events by combining estimates of the scaling function for rim heights with estimates of the scaling parameters for the average thickness of the ejecta blanket as a function of distance from the crater center.

Figure 4 is a plot of rim height (corrected for structural uplift) versus crater radius for cratering events spanning many decades of scale. Over limited ranges of crater size, the ejecta thickness at the crater rim can be approximated as a power law function of crater size. For the larger events, ranging from the larger nuclear explosion craters to the basin-forming impacts (McGetchin *et al.*, 1973), the data seem to be fit by the relationship  $T = 0.14 R^{0.74}$ , where  $T$  is ejecta thickness at the rim and  $R$  the crater radius (in meters). For smaller cratering events, such as those responsible for most of the regolithic mixing over the last few hundred million years, a different

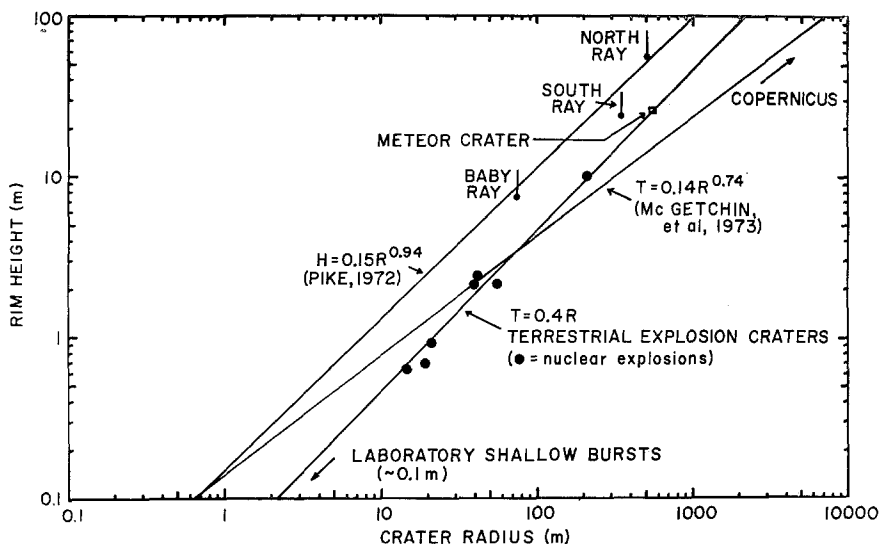


Fig. 4. Rim heights (corrected for structural uplift) versus radii for various impact and explosion craters. The scaling function for rim height of the largest terrestrial explosion craters and large lunar craters can be approximated by the relationship  $T=0.14R^{0.74}$ ; for terrestrial explosion craters and laboratory simulated cratering studies, it can be approximated by the relationship  $T=0.4R$ ; and small ( $<7$  km) lunar craters seem best approximated by the relationship  $T=0.10R^{0.94}$  (see text). Lines on the points for North Ray, South Ray, and Baby Ray show the effect of a 40% correction for structural uplift. Relationship of Pike (1972) describes the uncorrected rim height  $H$ .

functional relationship is indicated as shown by the results of laboratory simulations and terrestrial explosion craters ( $T=0.4R$ ). A closer examination, however, suggests that lunar impact craters and terrestrial explosion craters are sufficiently dissimilar that parameters for craters in the 10 cm to 1 km range cannot be adequately described by this relationship. Pike (1972) compiled data from a collection of nearly 500 lunar impact craters in the proper size interval from near-terminator Orbiter photography. These data also suggest a power law relationship between scale and rim heights which, fit to a least-squares line, provide the relationship  $H=0.15R^{0.94}$ , where  $H$  is the rim height (Pike, 1972). When corrected for a 40% structural uplift (Carlson and Jones, 1965), this becomes:

$$T = 0.10 R^{0.94}. \quad (2)$$

As can be seen from the points labeled 'North Ray', 'South Ray', and 'Baby Ray', the line is clearly compatible with the rim heights\* of these features. Vertical lines on the points indicate the extent of the corrections made for structural uplift. We feel that this line represents a more accurate relationship for lunar craters in the less than 1 km size range than do relationships derived for either the larger lunar craters or the terrestrial explosion and laboratory simulation craters.

\* Rim heights and crater profiles were obtained from AS11 stereo-plotter and mission pan photography prepared by the Mapping Sciences Branch, Earth Observation Division of JSC.



As pointed out by McGetchin *et al.* (1973), there is a substantial body of data suggesting that the ejecta thickness, as a function of distance from the crater, scales with crater radius  $R$  by the simple power law relationship

$$t = T \left( \frac{r}{R} \right)^{-3}, \quad (3)$$

where  $t$  is the ejecta thickness,  $T$  is ejecta thickness at the rim, and  $r$  is the range. Figure 3 shows some actual crater profiles, obtained from orbital pan photographs and the AS11 stereo-plotter,\* which tends to substantiate this relationship, at least on the continuous ejecta blanket. A combination of Equations (2) and (3) results in an expression for ejecta thickness as a function of crater size and range

$$t(r, R) = 0.10R^{0.94} (r/R)^{-3}, \quad (4)$$

which we can apply to the question of horizontal transport provided we know the relative frequency for the different sized cratering events. If  $dN$  is the number of craters per unit area with radii between  $R$  and  $R + dR$ , then the number of such craters in an annular ring of radius  $r$  and thickness  $dr$  will be given by  $2\pi r dr dN$ . The thickness of ejecta deposited from this ring is given by

$$2\pi r dr \int_0^r t(r, R) \frac{dN}{dR} dR,$$

where we limit the integration to craters of radius smaller than the radius of the annular ring. Therefore, the cumulative deposition of material originating from ranges greater than  $r$  is given by

$$T(>r) = \int_r^\infty 2\pi r' \int_0^{r'} t(r', R) \frac{dN}{dR} dR dr'. \quad (5)$$

Unless we have a saturated crater population, the relative frequency of cratering events of a given size range is proportional to the cumulative crater population in that size range. The cumulative crater population we have used, inferred from crater counts on production (non-saturated) surfaces, is given by  $N(>R) = KR^{-3.4}$  (Oberbeck *et al.*, 1973), where  $N(>R)$  is the number of craters of radius greater than  $R$ . Therefore,  $dN(R)$  is taken to be proportional to  $R^{-4.4} dR$  so that the relative transport of material from distances greater than  $r$  is given by

$$T(>r) \propto \int_r^\infty r'^{-2} \int_0^{r'} R^{0.46} dR dr' \propto r^{-0.46}. \quad (6)$$

\* Rim heights and crater profiles were obtained from AS11 stereo-plotter and mission pan photography prepared by the Mapping Sciences Branch, Earth Observation Division of JSC.

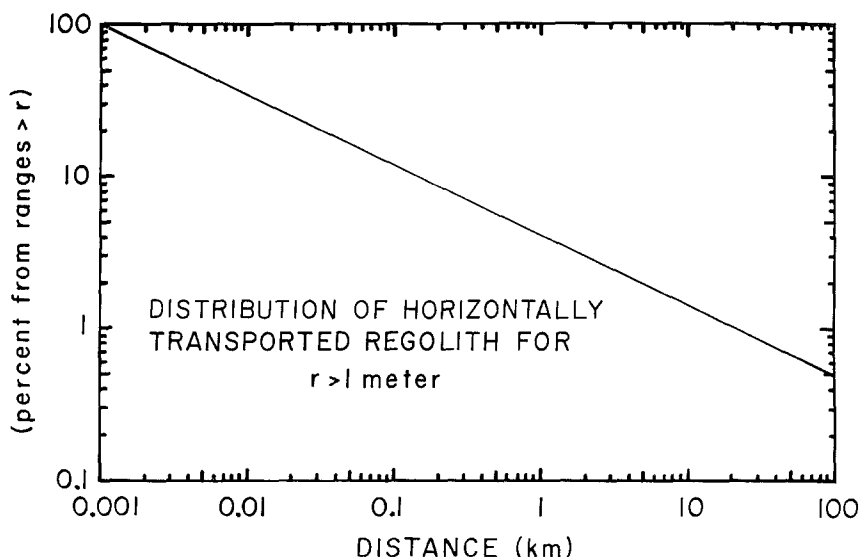


Fig. 5. Distribution of source ranges for the deposition of material horizontally transported by impact cratering over distances exceeding one meter. This distribution is defined by the relationship  $T(>r) = r^{-0.46}$  (see text).

Figure 5 is a plot of this function normalized to a one-meter range. It indicates that, of the material deposited from sources more than one meter away, about one percent will come from sources greater than 10 km away. The calculations are limited to horizontal transport over distances greater than one meter because ejecta systematics, developed for larger events, cannot be expected to hold over all size ranges and there is some evidence for anomalous lateral ejecta distributions for small-scale impacts in non-cohesive materials (Gault *et al.*, 1974). This range distribution is shallow enough to suggest that inter-regional mixing by impact ejection may be a significant mixing mechanism on the moon, but to adequately assess the process it is necessary to know something about the current meteoroid complex. Absolute cratering rates are much more elusive than relative cratering rates. Consequently, any computation based upon the absolute cratering rates should be taken, at best, as a factor of two or three estimate.

According to Oberbeck *et al.* (1973), three open maria regions of Oceanus Procellarum (Lunar Orbiter sites IIP11, IIP13b, and IIP7b) have cumulative crater populations described by  $N(>D) = KD^{-3.4}$ , where the values for  $K$  are respectively  $2.5 \times 10^7$ ,  $4.3 \times 10^7$ , and  $7.9 \times 10^7$ . (Note that the units are  $N$ , the number of craters per square kilometer, and  $D$ , the diameter in meters.) Events prior to 3.9 aeons probably included a large, and rapidly decaying (Shoemaker *et al.*, 1970), influx of projectiles bombarding the lunar surface as evidenced by comparative crater counts in mare and highland regions. Variable crater counts on the mare surfaces themselves may also be indicative that rapid changes in bombardment were occurring after basin formation. If this is true, one can argue that the region of Oceanus Procellarum with the lowest

crater count would be least affected by the enhanced early bombardment. We therefore adopt a cumulative crater population with  $K$  equal to  $2.5 \times 10^7$  for a surface 3.3 b.y. old and an average rate (craters per million years)  $dN/dt$  of  $7600D^{-3.4}$  fully realizing that, with the uncertainties in the past bombardment history, this value by itself may be only an order-of-magnitude estimate for current cratering rates. If the projectile flux did not fall rapidly at an early stage of maria evolution, but rather decreased slowly during the subsequent history, as suggested by Latham *et al.* (1972), a meaningful comparison between the present cratering rates and the long-term average rate calculated from the cumulative crater populations on Oceanus Procellarum cannot be made. A perhaps more accurate estimate of current cratering rates can be made from the cumulative crater populations on the floor and continuous ejecta blanket of Copernicus. If the age of Copernicus has been correctly inferred as 850 m.y. (Silver, 1971; Pepin *et al.*, 1972; Eberhardt *et al.*, 1973), crater counts should more accurately reflect current cratering rates. Greeley and Gault (1973) report cumulative crater populations on the ejecta blanket of Copernicus which, if interpreted in terms of the production function  $N(>R) = KD^{-3.4}$ , yield a value for  $K$  of  $6.3 \times 10^6$ . An average crater production rate (craters per million years)  $dN/dt$  of  $7400D^{-3.4}$  is found which is essentially identical to that derived from the Lunar Orbiter site IIIP11. This agreement would tend to argue against the influx model of Latham *et al.* (1972). More important here, however, is the added confidence it provides in current cratering rates, estimated now from a crater population developed only during the last billion years on Copernicus ejecta and consequently independent of the early bombardment history of the Moon. Putting this crater production function into Equation (5), now written in the form of a rate of accumulation of ejecta-derived deposits

$$\frac{dT}{dt}(>r) = \int_r^{\infty} 2\pi r' \int_0^{r'} t(r', R) \frac{d}{dR} \left( \frac{dN}{dt} \right) dR dr', \quad (7)$$

and integrating from  $r = 1$  m to  $\infty$ , we obtain a value of  $6 \text{ mm m.y.}^{-1}$  as the rate of deposition for material originating from sources one meter or more away. This rate of horizontal exchange, and the distribution of horizontally transported material shown in Figure 5, provide the means to examine the role that horizontal transport plays in lunar surface dynamics.

The extent to which horizontal exchange affects the rate and interpretation of soil maturation depends upon size of the regolith unit and the maturity of the surrounding regions. In the case of narrow ejecta rays deposited on older surfaces, maturation is probably dominated by horizontal mixing processes rather than the local production of agglutinates, solar flare tracks, and the other parameters used to describe soil maturity. Mixing times (to the 50% probability level) for soil columns one centimeter long have been estimated to be on the order of 5 m.y. by Monte Carlo methods of Gault *et al.* (1974) and others. We have estimated that the horizontal exchange of material with regions more distant than  $r$  (meters) occurs at a rate of about

$0.6r^{-0.46} \text{ cm m.y.}^{-1}$ . Equating these two mixing rates (horizontal interchange and vertical stirring), one comes to the general conclusion that, for horizontal scales much less than about 100 m, the mixing involves predominantly interchange with material from the surrounding regions. If the foreign material is mature, the apparent maturing rate will be governed almost entirely by the interchange rate. Therefore, the rates at which the albedo contrasts of ejecta rays disappear should inversely scale with the width of the ray, but values for the rates of degradation are difficult to predict since observable albedo differences may reflect only subtle differences in the apparent maturity.

To see what effect inter-unit mixing by impact transport has on apparent soil maturation for regions of larger size, we can compare the rates of apparent soil aging for both the intermixing and the local maturing processes. North Ray soils (particularly those of Station 11), being fairly young and part of a large continuous ejecta blanket, provide an estimate of the approximate rates of maturation by local processes. During a time characteristic of mixing to a 1 cm depth, roughly 5 m.y. (Gault *et al.*, 1974), about 10% of the grains accumulate a dose of solar flare tracks in excess of  $10^8 \text{ t cm}^{-2}$  (Figure 1). During this same time period the 90–150 $\mu$  soil fraction accumulates an agglutinate content of roughly 3% (Figure 2). Since the grains in fully matured soils are all track rich, there would only have to be an equivalent of about 0.2 mm m.y. $^{-1}$  of a fully matured soil component intermixed to completely mask the local maturing processes. The 90–150 $\mu$  fraction of mature soils seems to have an agglutinate content in excess of 50%. Only 0.1 m m.y. $^{-1}$  would therefore have to be stirred in to defeat the agglutinate criterion, although this is somewhat less certain since agglutinate destruction probably also accompanies cratering events. Since we estimate 0.06 mm m.y. $^{-1}$  as the characteristic horizontal exchange rate for ranges in excess of 10 km (Figure 5), it would appear that soil properties can be strongly influenced by components 10 km or more away.

All inter-unit mixing does not, of course, involve fully matured components. Ejecta derived from depth may be immature and, where the crater radius exceeds the regolith thickness, cratering will excavate fresh material. In addition, even though Equation (4) may more or less accurately approximates the mass distribution of ejecta from cratering events, the distribution of shocked, fragmented, melted, and material otherwise modified by the impact cannot be predicted from this treatment. For reasons such as these, the rate of maturation in the real world is a complicated set of processes, but inter-unit mixing seems to play a major role.

### Acknowledgments

We would like to acknowledge many helpful discussions with R. M. Walker, F. A. Podosek, and G. J. Taylor. Crater profiles were kindly provided by the Mapping Sciences Branch, Earth Observation Division, at JSC. We thank H. Ketterer for her fine work in preparation of the manuscript and B. Drozd for assistance with the drafting. We also thank staff of the Lunar Science Institute for help during visits by

Arvidson and Hohenberg. This work was partially supported by NASA Grant No. NSG 07016.

### References

- Alexander, E. C., Jr., Davis, P. K., Reynolds, J. H., and Srinivasan, B.: 1973, *Lunar Science IV*, 27–29.
- Arnold, J. R.: 1974, Talk presented at the Lunar Regolith Conference, Houston, Tex., 13–15 November.
- Arvidson, R., Crozaz, G., Drozd, R., Hohenberg, C., and Morgan, C.: 1975, *The Moon*, to be published.
- Behrmann, C., Crozaz, G., Drozd, R., Hohenberg, C., Ralston, C., Walker, R., and Yuhas, D.: 1973, *Proc. Fourth Lunar Sci. Conf.*, 1957–1974.
- Bogard, D. D. and Nyquist, L. E.: 1973, *Proc. Fourth Lunar Sci. Conf.*, 1975–1985.
- Carlson, R. H. and Jones, G. D.: 1965, *J. Geophys. Res.* **70**, 1897–1910.
- Clanton, U. S., McKay, D. S., Taylor, R. M., and Heiken, G. H.: 1972, *Apollo 15 Lunar Samples*, 54–56.
- Crozaz, G., Drozd, R., Hohenberg, C., Morgan, C., Ralston, C., Walker, R., and Yuhas, D.: 1974, *Proc. Fifth Lunar Sci. Conf.*, 2475–2499.
- Crozaz, G., Drozd, R., Graf, H., Hohenberg, C. M., Monnin, M., Ragan, D., Ralston, C., Seitz, M., Shirck, J., Walker, R. M., and Zimmerman, J.: 1972, *Proc. Third Lunar Sci. Conf.*, 1623–1636.
- Drozd, R. J., Hohenberg, C. M., Morgan, C. J., and Ralston, C.: 1974, *Geochim. Cosmochim. Acta* **38**, 1625–1642.
- Eberhardt, P., Geiss, J., Grogler, N., and Stettler, A.: 1973, *The Moon* **8**, 104–115.
- Gault, D. E., Hörz, F., Brownlee, D. E., and Hartung, J. B.: 1974, *Proc. Fifth Lunar Sci. Conf.*, 2365–2386.
- Greeley, R. and Gault, D. E.: 1973, *Earth Planetary Sci. Letters* **18**, 102–108.
- Heiken, G.: 1974, *A Catalog of Lunar Soils*, NASA Preprint, Johnson Space Center, Houston.
- Kirsten, T., Horn, P., and Kiko, J.: 1973, *Proc. Fourth Lunar Sci. Conf.*, 1757–1784.
- Latham, G. V., Ewing, M., Press, F., Sutton, G., Dorman, J., Nakamura, Y., Toksöz, N., Lammlein, D., and Duennbier, F.: 1972, *Apollo 16 Preliminary Science Report*, NASA SP-315, 9-1 to 9-29.
- McGetchin, T. R., Settle, M., and Head, J. W.: 1973, *Earth Planetary Sci. Letters* **20**, 226–236.
- McKay, D. S., Heiken, G. H., Taylor, R. M., Clanton, U. S., Morrison, D. A., and Ladle, G. H.: 1972, *Proc. Third Lunar Sci. Conf.*, 983–994.
- Marti, K. and Lightner, B. D.: 1972, *Science* **175**, 421–422.
- Maurette, M. and Price, P. B.: 1975, *Science* **187**, 121–129.
- Mitchell, J. K., Carrier, W. D. III, Costes, N. C., Houston, W. N., Scott, R. F., and Hovland, H. J.: 1973, *Apollo 17 Preliminary Science Report*, NASA SP-330.
- Muehlberger, W. R., Baston, R. M., Cernan, E. A., Freeman, V. L., Hait, M. H., Holt, H. E., Howard, K. A., Jackson, E. D., Larson, K. B., Reed, V. S., Rennilson, J. J., Schmitt, H. H., Scott, D. E., Sutton, R. L., Stuart-Alexander, D., Swann, G. A., Trask, N. J., Ulrich, G. E., Wilshire, H. G., and Wolfe, E. C.: 1973, *Apollo 17 Preliminary Science Report*, NASA SP-330.
- Mutch, T. A.: 1972, *Geology of the Moon*, (revised edition), Princeton Univ. Press, Princeton, N.J.
- Oberbeck, V. R., Quaide, W. L., Mahan, M., and Paulson, J.: 1973, *Icarus* **19**, 87–107.
- Oberbeck, V. R., Morrison, R. H., Hörz, F., Quaide, W. L., and Gault, D. E.: 1974, *Proc. Fifth Lunar Sci. Conf.*, 111–136.
- Pepin, R. O., Bradley, J. G., Dragon, J. C., and Nyquist, L. E.: 1972, *Proc. Third Lunar Sci. Conf.*, 1569–1588.
- Pike, R. J.: 1972, *Proc. Int. Geophys. Conf.*, 41–47.
- Reedy, R. C. and Arnold, J. R.: 1972, *J. Geophys. Res.* **77**, 537–555.
- Silver, L. T.: 1971, *Trans. Am. Geophys. Union* **52**, 534.
- Shoemaker, E. M., Hait, M. H., Swann, G. A., Schleicher, D. L., Schaber, G. G., Sutton, R. L., Dahlem, D. H., Goddard, E. N., and Waters, A. C.: 1970, *Proc. Apollo 11 Lunar Sci. Conf.*, 2399–2412.